HHS Public Access

Author manuscript

J Neuroimaging. Author manuscript; available in PMC 2015 December 13.

Published in final edited form as:

J Neuroimaging. 2015 ; 25(5): 844–847. doi:10.1111/jon.12206.

Magnetic Resonance Fiber Tracking in a Neonate with Hemimegalencephaly

Thomas J Re, **Laura Scarciolla**, **Emi Takahashi**, **Nicola Specchio**, **Bruno Bernardi**, and **Daniela Longo**

Boston Children's Hospital, Harvard Medical School - Radiology, Boston, MA (TJR); University Campus Biomedico – Radiology, Rome, Italy (LS); Boston Children's Hospital, Harvard Medical School – Division of Newborn Medicine, Department of Medicine, Fetal and Neonatal Imaging Science Center, Boston, MA (ET); Bambino Gesù Children's Hospital – Neurology, Rome, Italy (NS); and Bambino Gesù Children's Hospital – Neuroradiology, Rome, Italy (BB, DL).

Abstract

A magnetic resonance diffusion fiber tracking study in neonate diagnosed with left hemisphere hemimegalencephaly is presented. Despite diffuse morphologic deformities identified in conventional imaging, all major pathways were identifiable bilaterally with minor aberrations in vicinity of morphologic lesions.

Keywords

Hemimegaloencephaly; fiber tracking; neonate; MRI

Introduction

We present a magnetic resonance (MR) diffusion fiber tracking study in a neonate diagnosed with hemimegalencephaly. The patient, a preterm newborn (male; 37 weeks + 5 days), was admitted to the Neonatal Intensive Care Unit of Bambino Gesu' Pediatric Hospital in Rome for seizures appearing the first day of life. Clinical exam was unremarkable except for mild facial asymmetry. Electroencephalogram showed abnormal activity in the left temporal, parietal, and occipital lobes. Brain ultrasound imaging showed left-dominant volumetric asymmetry of the cerebral cortex.

Hemimegalencephaly is a rare malformation characterized by partial or whole enlargement of one cerebral hemisphere.[1] It is usually associated with abnormal gyration with variable types of cortical abnormalities in the affected hemisphere (pachygyria, polygyria, fused gyri, and shallow sulci), dilated or constricted ipsilateral ventricle with abnormally shaped frontal horn, neuronal heterotopia, thickening of the corpus callosum, and subcortical white matter signal abnormalities due to heterotopias, gliosis, and calcifications. In some cases, there is

Correspondence: Address correspondence to Thomas J Re, Boston Children's Hospital, 1 Autumn St, Room 456, Boston, MA 02115. drtjre@gmail.com.

Conflict of Interest: None.

hypertrophy of the ipsilateral brainstem and cerebellum abnormal architecture of the cerebellar folia, ipsilateral cranial nerve enlargement, and cerebral vascular dilatations.[2]

Few works have reported MR diffusion tractography findings in hemimegalencephaly and these have concentrated on interhemispheric and paramedian pathways. Kamiya et al[3] demonstrated the presence of aberrant midsagittal fibers and abnormally enlarged periventricular fibers while Takahashi et al[4] demonstrated corpus callosum asymmetry in hemimegalencephaly patients. We present a tractography study of major supra- and inferior tentorial pathways.

Methods

Conventional magnetic resonance imaging (MRI) (axial T1-TIR, T2-GRE, T2-TSE; coronal T2-TSE) with supplemental 64-direction diffusion-weighted MRI (b = 1,000 seconds/mm^2; one nondiffusion-weighted measurement b = 0 second/mm^2; repetition time (TR) = 10 seconds; echo time (TE) = 88 milliseconds; δ = 12.0 milliseconds; Δ = 24.2 milliseconds; field of view = 22 × 22 cm; slice thickness = 2.0 mm; matrix size = 128 × 128, integrated Parallel Acquisition Techniques (iPAT) = 2) was performed on a 3-T scanner (Siemens, Erlagen, Germany). DiffusionToolkit/TrackVis (trackvis.org) was used to reconstruct and visualize tractography pathways using a High Angular Resolution Diffusion Imaging (HARDI) algorithm with 45° threshold. A tractography atlas[5] was used to guide ROI placements in order to delineate principle brain pathways and represented graphically (Fig 2). Mean quantitative values of fractional anisotropy (FA), axial diffusion (AD), radial diffusion (RD), apparent diffusion coefficient (ADC), and volume of tracts per pathway were quantified bilaterally (Table 1). A tractography data set, acquired with similar technique, of age-matched nonpathologic neonates was used for qualitative comparison.

Results

Conventional MRI Findings

Conventional MRI (Fig 1) confirmed diffuse increase of volume in left cerebral hemisphere with abnormal gyral patterns, white matter heterogeneity, and blurring of the white-gray matter interface. The temporal and occipital lobes showed cortical thickening and polymicrogyria with white matter hypermylination as indicated by hyperintensity in T1-weighted imaging, and hypointensity in T2-weighted imaging. Lateral left ventricle showed posterior horn dilation and anterior horn collapse and straightening. Corpus callosum appeared dysmorphic.

Tractography Findings

Posterior Periventricular Pathways—Pathways just lateral to the posterior horns of the lateral ventricles (in vicinity of brain regions with the most evident alteration in T2W imaging) showed left-sided abnormality (Fig 2B: arrow-4) similarly to findings of Kamiya et al.[3] ADC_{mean}, RD_{mean}, and AD_{mean} were significantly lower on the left with overall increased FA_{mean}.

Corpus Callosum—The significant asymmetry of the callosum demonstrated by Takahashi[4] was not visible in our patient, although minor distortion was observed in posterior brain regions (Fig 2B: arrow-1).

Anterior Commissure—The anterior commissure pathways appeared slightly less robust in the hemimegaloencephalic neonate, particularly in the left hemisphere, when compared to the control (Fig 2C).

Cingulum—Cinguli pathways showed the most marked asymmetry among pathways studied. The left cingulum appeared sparse and fragmented (Fig 2B: arrow-2). ADC_{mean} and AD_{mean} were lower in the left pathway while RD_{mean} was substantially equivalent bilaterally. FA_{mean} resulted slightly lower on the left.

Fornix—The fornix was substantially symmetric and unremarkable.

Inferior Fronto-Occipital Fasciculus and Inferior Longitudinal Fasciculus—The inferior fronto-occipital fasciculus appeared comparable to that of the normal control (Fig 2A/B in cyan), while the inferior longitudinal fasciculus was sparse bilaterally (best viewed in Fig 2C in orange). Both pathways showed higher FA_{mean} and lower diffusivity (ADC_{mean}, AD_{mean}, RD_{mean}) on the left.

Uncinate—There was only slight volumetric asymmetry in the uncinate, similar to that described in nonpathological subjects.[6] FA_{mean} was higher while all other diffusivity values (ADC_{mean}, AD_{mean}, RD_{mean}) were lower on the left.

Corona Radiata (CR)—The CR appeared asymmetric. ADC_{mean} was substantially symmetric while FA_{mean} was higher and AD_{mean} and RD_{mean} were lower on the left. The left CR showed aberrant branching (Fig 2C: arrow-3), possibly reflecting altered cortical organization or the existence of pathologic regions causing the pathways to reroute.

Cerebellar Peduncle Tracks (CPTs)—All three CPTs demonstrated left-ward asymmetry in the patient, and sparsity of the left inferior peduncular track which are, however, also common findings in normal infants. The appearance of aberrant extension of the left superior cerebellar peduncle (SCP) track, as observed in this case (Fig 2D: arrow-5) is also common in normal subjects and likely an artifact. Mid-brain decussation of the SCP tracks were not detected on tractography; however, SCP and mid-brain structures appeared normal in T2W images (ie, no “molar-tooth”). In our experience, SCP track decussation is often not identified with the current tractography technique in normal subjects which may reflect limitations of the technique itself, likely not the true absence of such fibers as in the case of Jubert Syndrome.

Conclusions

Tractography generally reflected the conventional MR imaging, showing most important pathway aberration in the posterior regions of the left hemisphere. Interestingly, the quantitative diffusivity values (ADC, FA, AD, and RD) showed left-right variation in

structures which showed no apparent alteration on conventional imaging. In general, ADC was lower with FA higher in pathways in the enlarged left hemisphere. The factors influencing ADC and FA are very complex. Although such findings are compatible with hypermyelinization, they could also reflect increased cellular density due to increased neuronal compactness, gliosis, or heterotopias.[7] The exceptional case of lower left-sided FA found in the cingulum might be attributed to possible dysplastic development of this structure or its invasion by aberrant fibers of the adjacent corpus callosum. Both situations could theoretically lower the overall anisotropy of this structure, although other causes cannot be excluded.

One must not draw general conclusions concerning tractography in hemimegaloencephaly from a single case study; however, these results give hope that diffusion tractography and related quantities (ADC, FA, AD, and RD) may prove useful as indicators of the true extent of white matter alteration in this pathology and therefore merit further investigation.

Acknowledgments

This work was supported by the Ralph Schlaeger Fellowship Endowment Fund in Neuroimaging (TJR), and by the Eunice Shriver Kennedy National Institute of Child Health and Development (NICHD) (R01HD078561, R21HD069001) (ET).

References

1. Osborn, AG.; Salzam, KL.; Barkovich, AJ. Diagnostic Imaging:Brain. 2nd ed.. New York: Amirsys; 2009. p. 82-85.
2. Tortori-Donati, P.; Rossi, A. Pediatric Neuroradiology. 1st ed.. Heidelberg: Springer; 2005. p. 112-115.
3. Kamiya K, Sato N, Saito Y, et al. Accelerated myelination along fiber tracts in patients with hemimegalencephaly. J Neuroradiol. 2014 Jul; 41(3):202–210. [PubMed: 24091102]
4. Takahashi T, Sato N, Ota M, et al. Asymmetrical interhemispheric fiber tracts in patients with hemimegalencephaly on diffusion tensor magnetic resonance imaging. J Neuroradiol. 2009; 36(5): 249–254. [PubMed: 19783304]
5. Catani M, Thiebaut de Schotten M. A diffusion tensor imaging tractography atlas for virtual in vivo dissections. Cortex. 2008; 44(8):1105–1132. [PubMed: 18619589]
6. Wakana S, Caprihan A, Panzenboeck MM. Reproducibility of quantitative tractography methods applied to cerebral white matter. Neuroimage. 2007; 36(3):630–644. [PubMed: 17481925]
7. Salamon N, Andres M, Chute DJ, et al. Contralateral hemimicrencephaly and clinical-pathological correlations in children with hemimegalencephaly. Brain. 2006; 129(Pt 2):352–365. [PubMed: 16291806]

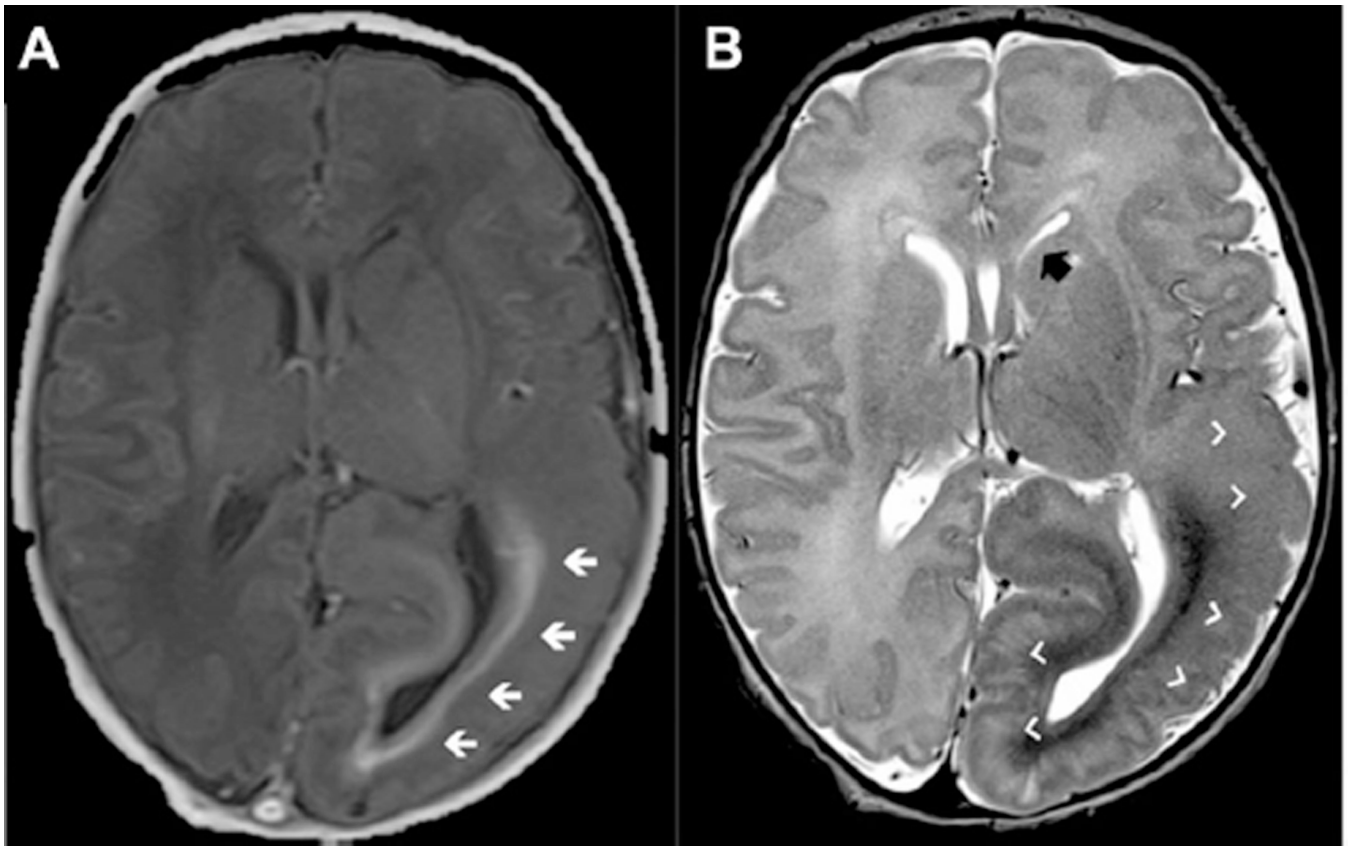

Fig 1.

Hemimegaloencephalic neonate: Conventional T1 (A) and T2 (B) imaging. Note, diffuse left hemispheric volume increase, abnormal gyral patterns, white matter heterogeneity, and blurring of the white-gray matter interface. Temporal and occipital lobes, in particular, showed cortical thickening and polymicrogyria (white arrow-heads). Also note lateral left ventricle anterior horn collapse (black-arrow).

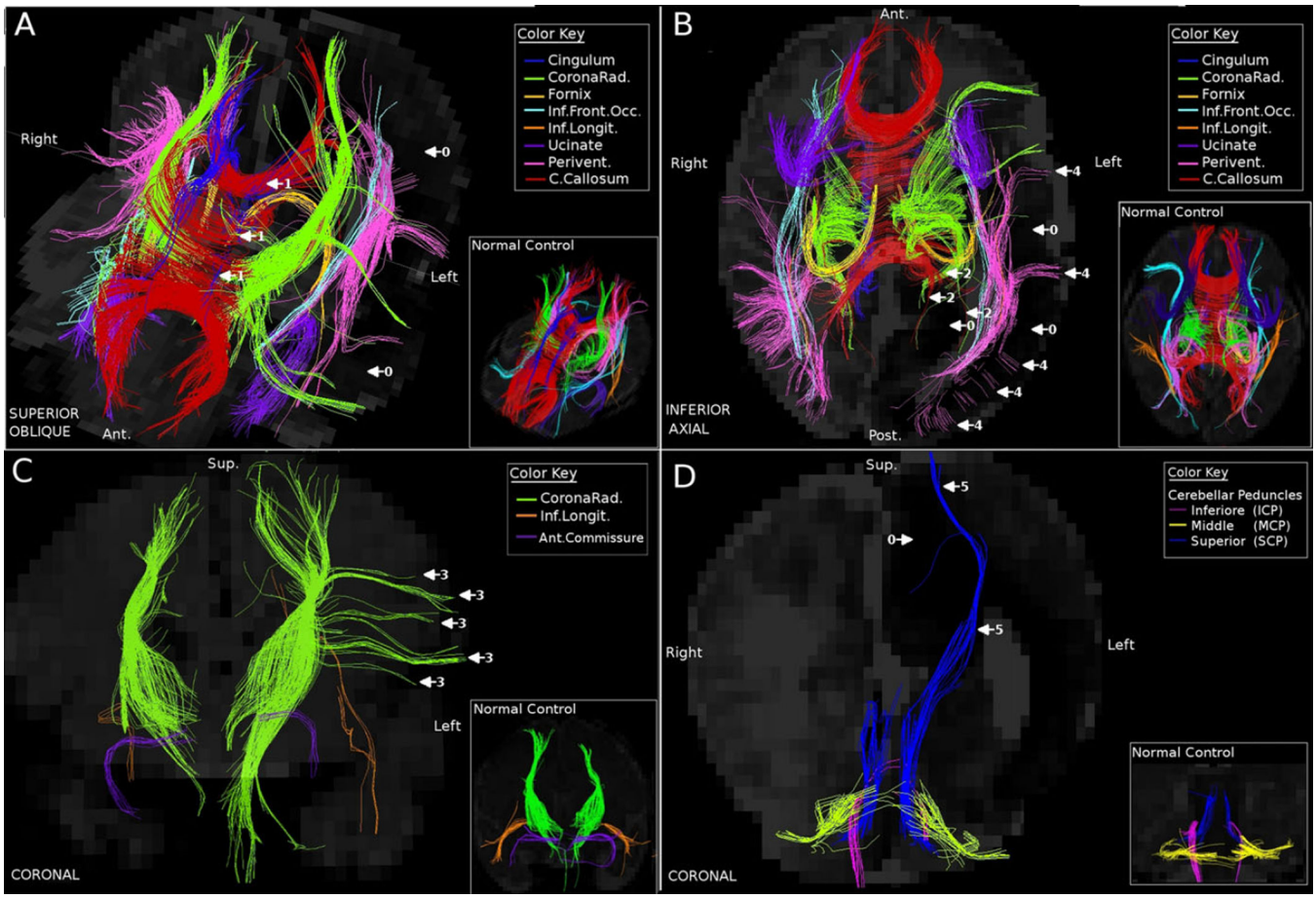

Fig 2.

Tractography graphical representation superimposed on T2W images. Supratentorial pathways seen from above (A) and below (B), select details (C). Cerebellar peduncular pathways (D) (arrows: 0-hypomylinated zones, 1-sparse/discontinuous left cingulum; aberrant branches of 2-callosum, 3-corona radiata, 4-periventricular, 5-sup.cerebellar peduncle). See text for other details.

Table 1

Track-based Quantitative Values for Left (Enlarged) and Right Brain of Hemimegaloencephaly Patient. Indicated for each track are: voxel volume, mean quantitative values of apparent diffusion coefficient (ADC), fractional anisotropy (FA), axial diffusivity (AD), and radial diffusivity (RD).

	Left (Enlarged) Hemisphere					Right Hemisphere				
	Voxels	**ADC × 10^{-3}**	**FA**	**AD × 10^{-3}**	**RD × 10^{-3}**	**Voxels**	**ADC × 10^{-3}**	**FA**	**AD × 10^{-3}**	**RD × 10^{-3}**
Cingulum	123	.72	.27	1.08	.00073	188	.92	.31	1.19	.00072
Corona radiata	1135	.88	.40	1.12	.00058	763	.84	.35	1.14	.00065
Fornix	107	.99	.32	1.59	.00095	122	.80	.33	1.31	.00077
Inf. fronto-occipital	182	.84	.44	1.07	.00053	308	1.26	.28	1.26	.00082
Inf. longitudinal	96	.88	.35	1.15	.00070	41	.92	.29	1.19	.00076
Paraventricolar	753	.90	.46	1.05	.00051	920	.97	.22	1.23	.00088
Ucinate	247	.85	.26	1.07	.00071	372	1.11	.24	1.17	.00080
Motor cortex	1351	.89	.44	1.00	.00051	544	.91	.29	1.12	.00071
SCP	221	1.45	.31	1.08	.00067	115	1.83	.25	1.20	.00082
MCP	192	1.48	.28	1.15	.00074	171	1.30	.29	1.13	.00070
ICP	18	2.14	.22	1.06	.00075	33	2.32	.28	1.20	.00079

*ADC, AD, RD in mm^2/seconds.